Vibrationally Quantum-State–Specific Reaction Dynamics of H Atom Abstraction by CN Radical in Solution

Stuart J. Greaves *et al.*

Science **331**, 1423 (2011);
DOI: 10.1126/science.1197796

Science (print ISSN 0036-8075; online ISSN 1095-9203) is published weekly, except the last week in December, by the American Association for the Advancement of Science, 1200 New York Avenue NW, Washington, DC 20005.

type observed in this work were concordantly predicted by numerous theoretical treatments. The result (*19*) on vortex-like domain structures in rhombohedral materials such as $BiFeO_3$ corroborates our observations in the epitaxial PZT-STO system. We would like to point out that the vortex-like domain structures brought about by the comparatively simple 180°-90°-180° domain arrangement of our work are observed in films of highly tetragonal $PbZr_{0.2}Ti_{0.8}O_3$, where polarization rotation might be considered less likely than in rhombohedral materials like $BiFeO_3$. Both studies show that in perovskite-oxide heterostructures, polarization-closure structures do occur. Our work demonstrates the unique capabilities of mapping of the dipole vector, unit cell by unit cell, by means of atomic-resolution TEM. This technique can therefore be used to study further details of domain structures close to interfaces in ferroelectric heterostructures and of vortex-like structures in ferroelectric materials. Because these structures are sensitive to the balance between competitive interactions, even small changes in the interface properties could have substantial effects on the depolarization field behavior. In fact, theory predicts striking effects for thicknesses on the order of a few nanometers in the PZT layer, where the top and bottom layers (metallic or insulating) cannot be treated separately (*10*). In addition, "dead" layers one unit cell thick (e.g., due to local deviations in permittivity caused by nonstoichiometry) are expected to change the flux-closure domain structure. Such investigations are also of potential importance for further progress in technology, in which increasingly thinner and smaller ferroelectric heterostructure systems are being considered for microelectronic applications.

References and Notes

1. M. E. Lines, A. M. Glass, *Principles and Applications of Ferroelectric and Related Materials* (Clarendon, Oxford, 1977).
2. J. F. Scott, *Ferroelectric Memories* (Springer, Berlin, 2000).
3. J. F. Scott, *Science* **315**, 954 (2007).
4. N. Setter, R. Waser, *Acta Mater.* **48**, 151 (2000).
5. K. Rabe, Ch. H. Ahn, J.-M. Triscone, Eds., *Physics of Ferroelectrics* (Springer, Berlin, 2007).
6. S. K. Streiffer *et al.*, *Phys. Rev. Lett.* **89**, 067601 (2002).
7. D. D. Fong *et al.*, *Science* **304**, 1650 (2004).
8. I. Kornev, H. Fu, L. Bellaiche, *Phys. Rev. Lett.* **93**, 196104 (2004).
9. B.-K. Lai, I. Ponomareva, I. Kornev, L. Bellaiche, G. Salamo, *Appl. Phys. Lett.* **91**, 152909 (2007).
10. S. Prosandeev, L. Bellaiche, *Phys. Rev. B* **75**, 172109 (2007).
11. P. Aguado-Puente, J. Junquera, *Phys. Rev. Lett.* **100**, 177601 (2008).
12. N. Balke *et al.*, *Nat. Nanotechnol.* **4**, 868 (2009).
13. L. J. McGilly, A. Schilling, J. M. Gregg, *Nano Lett.* **10**, 4200 (2010).
14. I. I. Naumov, L. Bellaiche, H. Fu, *Nature* **432**, 737 (2004).
15. I. Naumov, A. M. Bratkovsky, *Phys. Rev. Lett.* **101**, 107601 (2008).
16. A. Schilling *et al.*, *Nano Lett.* **9**, 3359 (2009).
17. B. J. Rodriguez *et al.*, *Nano Lett.* **9**, 1127 (2009).
18. Y. Ivry, D. P. Chu, J. F. Scott, C. Durkan, *Phys. Rev. Lett.* **104**, 207602 (2010).
19. C. T. Nelson *et al.*, *Nano Lett.* **11**, 828 (2011).
20. See supporting material on *Science* Online.
21. C. L. Jia, M. Lentzen, K. Urban, *Science* **299**, 870 (2003).
22. C. L. Jia *et al.*, *Nat. Mater.* **7**, 57 (2008).
23. K. W. Urban, *Science* **321**, 506 (2008).
24. C. L. Jia, L. Houben, A. Thust, J. Barthel, *Ultramicroscopy* **110**, 500 (2010).
25. M. Lentzen, *Microsc. Microanal.* **14**, 16 (2008).
26. C. L. Jia *et al.*, *Nat. Mater.* **6**, 64 (2007).
27. S. P. Alpay *et al.*, *J. Appl. Phys.* **85**, 3271 (1999).
28. I. Vrejoiu *et al.*, *Adv. Mater.* **18**, 1657 (2006).
29. B.-K. Lai *et al.*, *Phys. Rev. Lett.* **96**, 137602 (2006).
30. D. Lee *et al.*, *Phys. Rev. B* **80**, 060102(R) (2009).
31. G. B. Stephenson, K. R. Elder, *J. Appl. Phys.* **100**, 051601 (2006).
32. G. Herranz *et al.*, *Phys. Rev. B* **67**, 174423 (2003).
33. D. Toyota *et al.*, *Appl. Phys. Lett.* **87**, 162508 (2005).
34. J. Xia, W. Siemons, G. Koster, M. R. Beasley, A. Kapitulnik, *Phys. Rev. B* **79**, 140407(R) (2009).
35. Y. J. Chang *et al.*, *Phys. Rev. Lett.* **103**, 057201 (2009).

36. Supported by Deutsche Forschungsgemeinschaft grant SFB 762 (M.A., D.H., and I.V.).

Supporting Online Material

www.sciencemag.org/cgi/content/full/331/6023/1420/DC1
Materials and Methods
Fig. S1

18 November 2010; accepted 4 February 2011
10.1126/science.1200605

Vibrationally Quantum-State–Specific Reaction Dynamics of H Atom Abstraction by CN Radical in Solution

Stuart J. Greaves,[1] Rebecca A. Rose,[1] Thomas A. A. Oliver,[1] David R. Glowacki,[1] Michael N. R. Ashfold,[1] Jeremy N. Harvey,[1] Ian P. Clark,[2] Gregory M. Greetham,[2] Anthony W. Parker,[2] Michael Towrie,[2] Andrew J. Orr-Ewing[1]*

Solvent collisions can often mask initial disposition of energy to the products of solution-phase chemical reactions. Here, we show with transient infrared absorption spectra obtained with picosecond time resolution that the nascent HCN products of reaction of CN radicals with cyclohexane in chlorinated organic solvents exhibit preferential excitation of one quantum of the C-H stretching mode and up to two quanta of the bending mode. On time scales of approximately 100 to 300 picoseconds, the HCN products undergo relaxation to the vibrational ground state by coupling to the solvent bath. Comparison with reactions of CN radicals with alkanes in the gas phase, known to produce HCN with greater C-H stretch and bending mode excitation (up to two and approximately six quanta, respectively), indicates partial damping of the nascent product vibrational motion by the solvent. The transient infrared spectra therefore probe solvent-induced modifications to the reaction free energy surface and chemical dynamics.

In a chemical reaction, the partitioning of energy between translational, rotational, vibrational, and electronic degrees of freedom of the products depends on, and therefore provides information about, the potential energy landscape over which bonding changes occur (*1*). Early insights came from Polanyi (*2*), who demonstrated the importance of the location of an energy barrier along a reaction pathway in determining the fraction of the available energy that is released as product vibrational excitation. An expanding array of experimental techniques, complemented by theory, is enabling study of the dynamics of reactions in ever-increasing detail under low-pressure, gas-phase conditions in which the molecules are largely isolated from collisions and from the perturbations of a surrounding medium such as a solvent (*1*, *3*–*5*).

Much synthetic, environmental, and biological chemistry occurs in solution, however, and the solvent will have a pronounced effect on the dynamics of chemical reactions (*6*–*8*). The very short time intervals between collisions in the liquid phase, and the hindered motions of molecules surrounded by a solvent cage, prevent application of many of the velocity- and quantum-state–specific experimental methods developed to examine gas-phase collisions (*9*). Spectroscopic methods using ultrafast lasers can be used to measure the time scales for reactions in solution (*10*–*13*), study solvent-solute complexes (*14*, *15*), and examine molecular vibrational excitation, which can persist in solution for tens or hundreds of picoseconds (*16*). For a solution-phase bimolecular reaction, observation of vibrational quantum-state–specific energy disposal might provide comparable mechanistic insight to the infrared (IR) chemiluminescence (*1*, *2*) and more recent velocity-map imaging (*3*) studies of gas-phase reactions and therefore unravel the influence of the solvent on the dynamics. This prospect was recognized by Hochstrasser and co-workers (*10*, *11*), who used transient IR absorption to examine the products of reactions of Cl atoms or CN radicals with organic solvents. These pioneering experiments provided evidence that ~20% of the DCN products of the CN reaction with $CDCl_3$ solvent are formed with one quantum of vibrational excitation in the C-D stretching mode.

Here, experimental outcomes are presented for a solution-phase bimolecular reaction, which demonstrate a much greater degree of product vibra-

[1]School of Chemistry, University of Bristol, Cantock's Close, Bristol BS8 1TS, UK. [2]Central Laser Facility, Research Complex at Harwell, Science and Technology Facilities Council, Rutherford Appleton Laboratory, Harwell Science and Innovation Campus, Didcot, Oxfordshire, OX11 0QX, UK.

*To whom correspondence should be addressed. E-mail: a.orr-ewing@bris.ac.uk

tional excitation than was reported in prior studies of related reactions (*10*, *14*, *15*). As a consequence, vibrational mode–specific dynamics can be explored and are shown to be affected, but not quenched, by the presence of a solvent. The reaction of CN radicals with cyclohexane (Eq. 1),

$$CN + c\text{-}C_6H_{12} \rightarrow HCN + c\text{-}C_6H_{11} \quad (1)$$

and its deuterated counterpart are sufficiently exothermic that several vibrationally excited levels of the HCN (DCN) products are energetically accessible. Indeed, experimental studies of the gas-phase reactions of CN with small alkanes demonstrate efficient channeling of energy into as many as 6 quanta of the bending and 2 quanta of the C-H stretching vibrational modes of the HCN products (*17*–*21*). The three vibrational modes of HCN are well-described as a C-N stretch (ν_1), a bend (ν_2), and a C-H stretch (ν_3) (*22*), and are all IR active. These reactions therefore offer scope to examine how a liquid solvent alters the chemical dynamics by contrasting the nature and extent of vibrational excitation of the products in solution with the outcomes of gas-phase reactive collisions.

We obtained transient IR spectra with picosecond time resolution using the ULTRA laser facility at the Rutherford Appleton Laboratory (*23*). Figure 1 shows IR absorption spectra recorded at various time delays (≤400 ps) after narrow-bandwidth IR excitation of the C-H or C-N stretching vibration of HCN in solution in CH_2Cl_2. The spectra were obtained with broadband (~500 cm^{-1}) IR probe pulses and are a necessary precursor to the chemical reaction studies described later because they identify unambiguously the locations of bands of vibrationally excited molecules and their relaxation rates in solution. The features centered at 3263 and 3160 cm^{-1} are assigned, respectively, to the $v = 0 \rightarrow v_3 = 1$ and $v_3 = 1 \rightarrow v_3 = 2$ bands of HCN, hereafter denoted by 3_0^1 and 3_1^2, respectively (*24*), and the features at 2094 and 2073 cm^{-1} are the 1_0^1 and 1_1^2 bands, respectively. The negative-going signals for the 3_0^1 band correspond to a bleach in the vibrational ground-state population that recovers through vibrational relaxation, and the positive-going signals for the 3_1^2 band derive from a transient population of $v_3 = 1$ that relaxes back to the ground state (*25*). Similar descriptions apply to the spectra of the 1_0^1 and 1_1^2 bands. Fits of the time-dependence of the integrated intensities of the 3_1^2 bands to bi-exponential functions yield time constants for the relaxation of HCN($v_3 = 1$) and recovery of HCN($v = 0$) in $CHCl_3$, CH_2Cl_2, and $CDCl_3$ of 130 ± 5, 144 ± 8, and 265 ± 20 ps, respectively. Corresponding analysis of the 1_1^2 band gives time constants for relaxation of the C-N stretch in these same three solvents of 157 ± 38, 146 ± 17, and 122 ± 20 ps. All uncertainties are 1 SD from fits to 3 to 6 data sets.

The results of reactive experiments for CN radicals, initiated by 266-nm, ~50-fs ultraviolet (UV) laser photolysis of ICN (0.14 M) in the presence of cyclohexane (1.0 M) in CH_2Cl_2 solvent are shown in Fig. 2. The ultrafast dynamics of ICN photolysis in solution have previously been well characterized (*26*, *27*). The spectra in the C-H stretching region show formation of both vibrationally excited and ground-state HCN products. The majority of the signal derives from reaction (1), with a weak contribution from reaction of CN radicals with the solvent, as shown in Fig. 2, bottom. The main bands occur at the same wavenumbers as those in Fig. 1A and are assigned as the 3_1^2 and 3_0^1 transitions of HCN,

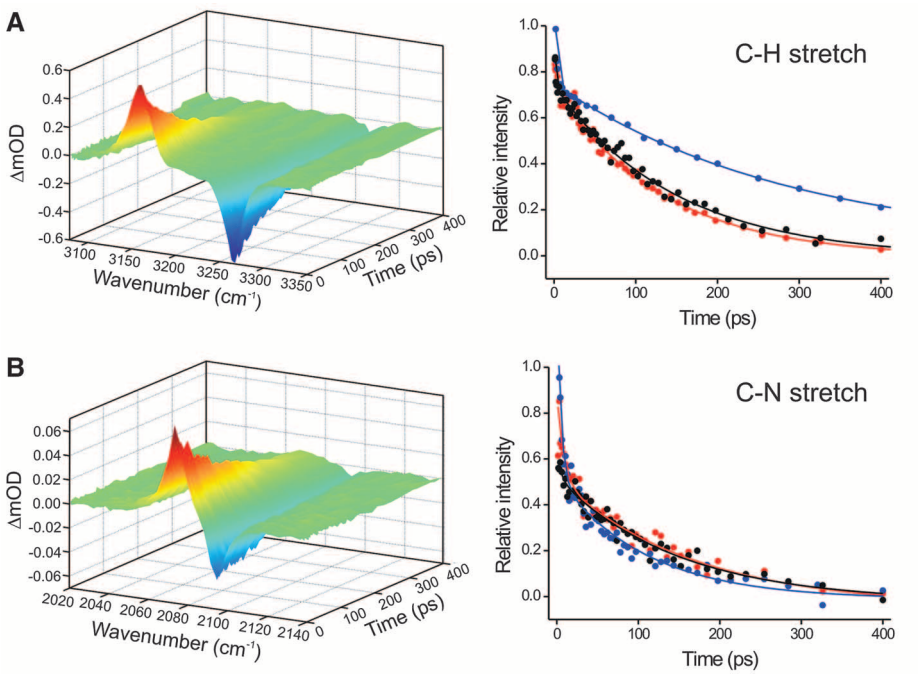

Fig. 1. Transient IR spectra of HCN in solution in CH_2Cl_2 (left) showing the temporal behavior in the (**A**) C-H and (**B**) C-N stretching regions after IR excitation on the fundamental absorptions (*25*). The right-hand plots show the time-dependence of the integrated intensities of the hot-band spectral features in three solvents, CH_2Cl_2 (black), $CHCl_3$ (red), and $CDCl_3$ (blue), with bi-exponential fits to extract time constants; the fast and slow decay components correspond respectively to rotational diffusion and vibrational relaxation.

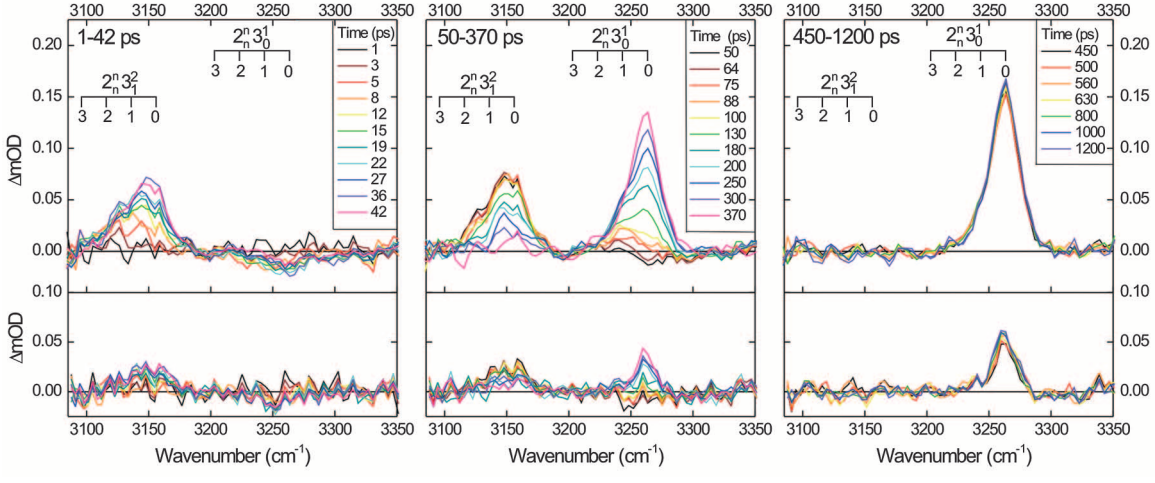

Fig. 2. Transient IR spectra, obtained in the C-H stretching region, of HCN products of UV-laser–initiated CN reactions in a 1.0 M solution of cyclohexane in CH_2Cl_2 (top row) and pure CH_2Cl_2 (bottom row). The combs above the spectra indicate spectroscopic assignments as described in the text. The spectra are displayed in time intervals selected to highlight the evolution from vibrationally excited to ground-state HCN (*25*).

but additional features appear to the low wavenumber side of the main bands. These shoulders are assigned to diagonal hot bands in the HCN-bending vibration (2^n_n, with $n \geq 1$ denoting the number of quanta of excitation of the bend) observed in combination with the C-H stretching transitions. These $2^n_n3^2_1$ and $2^n_n3^1_0$ combination bands are slightly displaced from the 3^2_1 and 3^1_0 features by anharmonic shifting of the C-H stretching frequency and are observed because the reaction deposits energy in the HCN bending vibrational mode. The 3^2_1 and $2^n_n3^2_1$ bands rise in intensity at earlier times than do the 3^1_0 and $2^n_n3^1_0$ bands, but the 3^1_0 band becomes the sole spectral feature at longer time delays (*25*). Reaction (1) was also studied in $CDCl_3$, which will exhibit different couplings to the reaction path and product motions, and similar HCN vibrational dynamics were observed (*28*). These observations are clear signatures that the reaction dynamics preferentially form HCN vibrationally excited with one quantum of C-H stretching motion and up to two quanta of bending excitation, followed by vibrational relaxation to the ground state by coupling to the solvent bath. Weakly negative signals on the 3^1_0 band at early times are a consequence of a population inversion between $v_3 = 1$ and $v = 0$ vibrational levels. There is no evidence for the formation of HCN in higher vibrational levels of the C-H stretching and bending modes: The combs in Fig. 2 indicate where absorption features involving $v_2 = 3$ are expected, but these and the 3^3_2 band were not observed. Signal-to-noise ratios suggest an upper limit of 10% branching into $v_2 \geq 3$ and $v_3 \geq 2$ products.

The spectra for different pump-probe time delays were fitted to six Gaussian functions with centers fixed to the central wavenumbers of the $2^n_n3^2_1$, 3^2_1, $2^n_n3^1_0$, and 3^1_0 bands ($n = 1$ and 2) and widths constrained to that of the 3^1_0 band at large time delays. For reaction (1) in CH_2Cl_2, Fig. 3 displays the time-dependence of the resultant integrated peak areas. The $2^n_n3^2_1$ intensity data have been combined, as have the intensities of the $2^n_n3^1_0$ bands, and the weak contribution from reaction with the solvent has been subtracted.

The time-dependent data were fitted to a kinetic model that incorporated reaction to form nascent HCN(0n1), HCN(001), HCN(0n0), and HCN(000) with respective pseudo-first-order rate coefficients (*29*) k_1, k_2, k_3, and k_4. The terms in parentheses denote numbers of quanta of excitation of the modes ($v_1v_2v_3$). The model also included vibrational relaxation in steps of a single quantum (with rate coefficients k_4 to k_8). It has analytical solutions for the time dependence of the concentrations of HCN($0v_2v_3$) to which the data were simultaneously fit. Allowance was made for the dependence of IR absorption signals on the population difference between levels connected by a spectroscopic transition, and the fits incorporated differences in the transition dipole moments for HCN with zero and one quanta of C-H stretch (*30*). The fits were further constrained by fixing the rate coefficients for loss of a quantum of C-H stretch to the values derived from the IR-pump-and-probe experiments for HCN in CH_2Cl_2. Fitted values of k_1 through k_4 are displayed in Fig. 3 and can be interpreted as being proportional to the reactive branching to form nascent HCN(0n1), HCN(001), HCN(0n0), and HCN(000) products. The values indicate that the reaction preferentially forms HCN with a quantum of C-H stretch and additional bending excitation ($v_2 \leq 2$); the main source of population of HCN(000) is through vibrational relaxation by coupling to the solvent over time scales of ~130 to 270 ps.

Reactions of CN with alkanes release ~10000 cm^{-1} of energy, and experimental investigations of such reactions in the gas phase (*17*–*21*) demonstrated that the excess energy is efficiently coupled into certain internal motions of the products: There is substantial excitation of both the HCN bending mode (up to $v_2 \sim 6$) and the C-H stretching mode ($v_3 \leq 2$). Our quasi-classical trajectory calculations for isolated reactive collisions indicate that the bending excitation of the HCN stems from a flat bending potential in the vicinity of the transition state (TS) (*31*), although the high rotational excitation of CN radicals from UV photo-

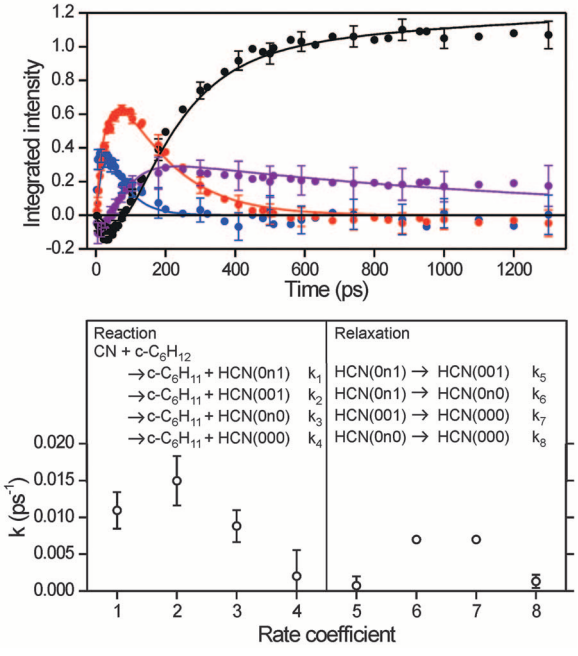

Fig. 3. (**Top**) The time-dependence of the integrated intensities of spectral bands in the C-H stretching region of HCN formed from reaction (1) in solution in CH_2Cl_2: Blue is HCN(0n1) (n = 1,2), red is HCN(001), purple is HCN(0n0), and black is HCN(000). Solid lines show fits to the (**Bottom**) summarized kinetic model , which also displays values of the rate coefficients obtained for each step. Error bars on individual data points are ±2 SD from the least-squares fitting to band intensities; uncertainties in rate coefficients are 1 SD from fits to four data sets.

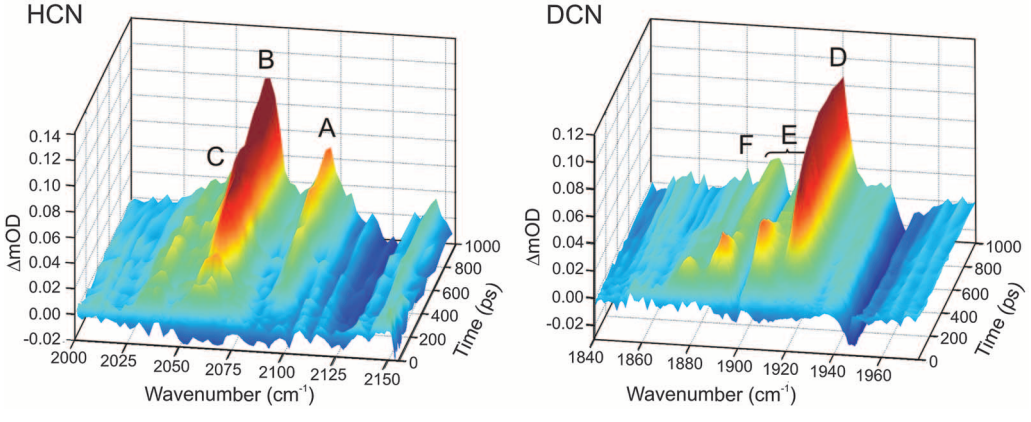

Fig. 4. Time-dependent IR spectra obtained in the C-N stretching regions of HCN and DCN for UV-laser–initiated CN reactions with c-C_6H_{12} in CH_2Cl_2 and c-C_6D_{12} in $CHCl_3$. Features (**A**) and (**D**) are the 1^1_0 bands in HCN and DCN, respectively. Bands (**B**) and (**C**), centered at 2065 and 2037 cm^{-1}, are assigned, respectively, to INC and to CN radicals, which may be complexed with the solvent. For HCN, hot bands of v_1 and combinations of the 1^1_0 transition with hot bands of the other two modes overlap band (B); for DCN, these bands are in the region indicated as (**E**). Band (**F**) is discussed in the text. The dips in the DCN spectrum at 1899 [at the center of region (E)] and 1946 cm^{-1} are solvent absorption–induced transient signals (*25*).

dissociation of ICN (*26*) may contribute. Early H-atom transfer at an extended C-H distance causes the observed excitation in the C-H stretching mode. The condensed phase experiments observe lower vibrational excitation of HCN than was reported for isolated collisions in the gas phase, however. We deduce that the solvent partially suppresses the flow of the excess energy of the reaction into product vibration, but that despite the presence of the solvent, many features of the dynamics on an attractive potential energy surface with an early barrier and loose bending potential persist. Calculations indicate that the location of the TS is not much affected by solvation, and the reduction in the vibrational content of the HCN therefore derives from solvent friction in the post-TS region (*31*).

Figure 4 shows transient IR spectra in the C-N stretching region of HCN and DCN products from CN radical reaction with c-C_6H_{12} in CH_2Cl_2 and c-C_6D_{12} in $CHCl_3$, respectively. Spectral features are assigned to the 1_0^1 C-N fundamental band and, at early times, to bands involving this transition in combination with hot bands in the bending and C-H (or C-D) stretching vibrations (in accord with the aforementioned promotion of excitation in these modes by the chemical dynamics). For the CN + c-C_6H_{12} reaction, there is no firm evidence of excitation of the C-N stretch in the HCN product, but analysis is complicated by features at 2065 and 2037 cm^{-1} assigned, respectively, to INC (*32*) and CN [either as free radicals in solution or weakly complexed with solvent molecules (*14*, *15*)]. The C-N stretching region of DCN is free from the above interferences, and an additional, weak transient feature (Fig. 4F) is seen at 1877 cm^{-1}. A plausible assignment to the $1_1^2 3_1^1$ or $1_1^2 2_n^n 3_1^1$ combinations of hot bands is consistent with the reaction dynamics channeling energy into the C-D stretching and bending motions but also indicates some C-N stretching activity in reactions forming DCN. This latter observation may be a consequence of subtly different reaction dynamics for the D-atom abstraction or more mixed C-D and C-N stretching character of the normal vibrational modes of DCN.

In conclusion, transient IR absorption spectroscopy has shown that the dynamics of the reactions of CN radicals with cyclohexane in chlorinated solvents have many features in common with their gas-phase counterparts. The HCN products are formed with high degrees of vibrational excitation (on average, ~30% of the available energy), and ground-state HCN mostly results from vibrational relaxation via coupling to the solvent on a slower time scale. The dynamics are vibrationally quantum-state–specific, with preferential excitation of a single quantum of the C-H stretching mode and up to two quanta in the bending mode. This degree of vibrational excitation is, however, lower than has been reported for comparable reactions in the gas phase, indicating partial damping of the developing HCN vibrational motion after the transition state. The transient IR spectra illustrate a strategy to explore not only the ways in which a solvent modifies the potential energy landscape for a chemical reaction in solution but also constrains the chemical reaction dynamics.

References and Notes

1. R. D. Levine, *Molecular Reaction Dynamics* (Cambridge Univ. Press, Cambridge, 2005).
2. J. C. Polanyi, *Acc. Chem. Res.* **5**, 161 (1972).
3. S. J. Greaves, R. A. Rose, A. J. Orr-Ewing, *Phys. Chem. Chem. Phys.* **12**, 9129 (2010).
4. X. Yang, *Annu. Rev. Phys. Chem.* **58**, 433 (2007).
5. S. C. Althorpe, D. C. Clary, *Annu. Rev. Phys. Chem.* **54**, 493 (2003).
6. J. F. Cahoon, K. R. Sawyer, J. P. Schlegel, C. B. Harris, *Science* **319**, 1820 (2008).
7. O. F. Mohammed, D. Pines, J. Dreyer, E. Pines, E. T. J. Nibbering, *Science* **310**, 83 (2005).
8. A. E. Bragg, W. J. Glover, B. J. Schwartz, *Phys. Rev. Lett.* **104**, 233005 (2010).
9. G. A. Voth, R. M. Hochstrasser, *J. Phys. Chem.* **100**, 13034 (1996).
10. D. Raftery, E. Gooding, A. Romanovsky, R. M. Hochstrasser, *J. Chem. Phys.* **101**, 8572 (1994).
11. D. Raftery, M. Iannone, C. M. Phillips, R. M. Hochstrasser, *Chem. Phys. Lett.* **201**, 513 (1993).
12. C. G. Elles, F. F. Crim, *Annu. Rev. Phys. Chem.* **57**, 273 (2006).
13. L. Sheps, A. C. Crowther, S. L. Carrier, F. F. Crim, *J. Phys. Chem. A* **110**, 3087 (2006).
14. A. C. Crowther, S. L. Carrier, T. J. Preston, F. F. Crim, *J. Phys. Chem. A* **112**, 12081 (2008).
15. A. C. Crowther, S. L. Carrier, T. J. Preston, F. F. Crim, *J. Phys. Chem. A* **113**, 3758 (2009).
16. J. C. Owrutsky, D. Raftery, R. M. Hochstrasser, *Annu. Rev. Phys. Chem.* **45**, 519 (1994).
17. G. A. Bethardy, F. J. Northrup, R. G. Macdonald, *J. Chem. Phys.* **102**, 7966 (1995).
18. G. A. Bethardy, F. J. Northrup, R. G. Macdonald, *J. Chem. Phys.* **105**, 4533 (1996).
19. L. R. Copeland, F. Mohammad, Z. Mansour, D. H. Volman, W. M. Jackson, *J. Chem. Phys.* **96**, 5817 (1992).
20. V. R. Morris, F. Mohammad, L. Valdry, W. M. Jackson, *Chem. Phys. Lett.* **220**, 448 (1994).
21. C. Huang, W. Li, A. D. Estillore, A. G. Suits, *J. Chem. Phys.* **129**, 074301 (2008).
22. G. Herzberg, *Molecular Spectra and Molecular Structure volume II, Infrared and Raman Spectra of Polyatomic Molecules* (Van Nostrand Reinhold Company, New York, 1945).
23. G. M. Greetham *et al.*, *Appl. Spectrosc.* **64**, 1311 (2010).
24. In the vibrational band notation, the main digit specifies the vibrational mode (1 = C-N stretch, 2 = bend, and 3 = C-H or C-D stretch), and the sub- and superscripts indicate, respectively, the number of quanta of vibration in the lower and upper levels connected by the IR transition.
25. Animated versions of time-dependent spectra are available in the supporting online material.
26. A. C. Moskun, S. E. Bradforth, *J. Chem. Phys.* **119**, 4500 (2003).
27. A. C. Moskun, A. E. Jailaubekov, S. E. Bradforth, G. Tao, R. M. Stratt, *Science* **311**, 1907 (2006).
28. Transient IR spectra for HCN products of reaction (1) in $CDCl_3$ are shown in the supporting online material.
29. For reactions of CN radicals with cyclohexane, the cyclohexane is in large excess and pseudo-first-order kinetic analysis can be used. Similarly, for the vibrational relaxation steps the solvent is in excess over other components of the system and is the dominant quencher.
30. P. Botschwina, *Chem. Phys.* **81**, 73 (1983).
31. Materials and methods are available as supporting material on *Science* Online.
32. NIST Chemistry Webbook, NIST Standard Reference Database Number 69, P. J. Linstrom, W. G. Mallard, Eds. (National Institute of Standards and Technology, Gaithersburg, MD, 20899); available at http://webbook.nist.gov; retrieved 15 September 2010.

33. Measurements were made at the Central Laser Facility, Rutherford Appleton Laboratory, with financial support for the ULTRA laser complex from the Science and Technology Facilities Council (STFC) and UK Biotechnology and Biological Sciences Research Council (STFC Facility Grant ST/501784). Funding for the Bristol group was provided by the Engineering and Physical Sciences Research Council Programme Grant EP/G00224X. We thank the Leverhulme Trust for an Early Career Research Fellowship (S.J.G.) and the Royal Society and the Wolfson Foundation for a Research Merit Award (A.J.O.E.).

Supporting Online Material

www.sciencemag.org/cgi/content/full/science.1197796/DC1
Materials and Methods
Figs. S1 to S5
Table S1
References
Movies S1 to S5

15 September 2010; accepted 20 January 2011
Published online 3 February 2011;
10.1126/science.1197796

Regeneration of Ammonia Borane Spent Fuel by Direct Reaction with Hydrazine and Liquid Ammonia

Andrew D. Sutton,[1]* Anthony K. Burrell,[2] David A. Dixon,[3] Edward B. Garner III,[3] John C. Gordon,[1]* Tessui Nakagawa,[2] Kevin C. Ott,† J. Pierce Robinson,[3] Monica Vasiliu[3]

Ammonia borane (H_3N-BH_3, AB) is a lightweight material containing a high density of hydrogen (H_2) that can be readily liberated for use in fuel cell–powered applications. However, in the absence of a straightforward, efficient method for regenerating AB from dehydrogenated polymeric spent fuel, its full potential as a viable H_2 storage material will not be realized. We demonstrate that the spent fuel type derived from the removal of greater than two equivalents of H_2 per molecule of AB (i.e., polyborazylene, PB) can be converted back to AB nearly quantitatively by 24-hour treatment with hydrazine (N_2H_4) in liquid ammonia (NH_3) at 40°C in a sealed pressure vessel.

A critical factor in realizing a hydrogen (H_2) economy is storage of the molecule for controlled delivery, presumably to an energy-producing fuel cell (*1*). Options for H_2 storage include compressed hydrogen, metal hydrides (*2*), and porous sorbent materials (*3*). In addition